Π-shaped Coiled Stator Ultrasound Motor for Rotating Ultrasound Sensor in Intravascular Ultrasound Imaging

Toshinobu Abe, Shinichi Takeuchi
Graduate School of Engineering
Toin University of Yokohama
Yokohama-shi, Japan
b22c003n@ust.toin.ac.jp

Tadashi Moriya
Professor Emeritus
Tokyo Metropolitan University
Hino-shi, Japan

Takasuke Irie, Masakazu Satou
Microsonic Co., Ltd.
Kokubunji-shi, Japan

***Abstract*—The primary focus of this paper is the development of an ultra-miniature ultrasound motor for rotating the ultrasound sensor in an intravascular ultrasonography (IVUS) system for use in the human blood vessel. Recently, intravascular diagnosis by IVUS has become widely used in medicine. IVUS is minimally invasive and can reduce pain felt by the patient, and is mainly used for examination of coronary artery disease. Since the size of the drive source for rotating the ultrasound sensor is large in the IVUS systems currently in practical use, it is installed outside the body, and the rotational power for the ultrasound sensor is transmitted through the long tortuous blood vessel. Such systems suffer from the problem that the rotation becomes non-uniform due to overloading of the wire transmitting the rotational power, and the problem that the available time is limited in order to prevent the wire from being damaged by overloading. We have therefore developed a Π-shaped coiled stator ultrasound motor (CS-USM) as a miniature ultrasound motor for rotating the ultrasound sensor for use in blood vessels in order to solve these problems. The CS-USM will achieve stable rotation of the ultrasound sensor in the blood vessel, since there is no need to transfer the rotational power though the long tortuous blood vessel. Furthermore, damage to the wire due to overloading is expected to be prevented. In this paper, we describe measurement of the torque, revolution speed, output power, and efficiency of the Π-shaped CS-USM.**

Keywords-CS-USM; Coiled stator; Ultrasound; Motor; Closed-loop waveguide; Revolution speed; Torque

I. INTRODUCTION

Recently, intravascular surgery and diagnosis have been used in medicine, for example, in atherectomy and IVUS. Intravascular surgery is a minimally invasive surgical method. Atherectomy is a method for removing atherosclerosis from blood vessels [1]. IVUS is mainly used to observe the luminal area and to confirm coronary stent expansion. IVUS visualizes the tissue beneath the surface, which is not possible by optical angiography [2] [3]. These devices need to perform rotational movement within the vessel.

The device that drives the revolution, such as a motor, is located outside the body in the IVUS systems currently in practical use. Non-uniform rotation and breakage of the shaft that transmits the rotational motion can occur due to undesired mechanical loading in long tortuous blood vessels. A small motor that can be used within the blood vessels is therefore needed in order to overcome these problems. A small motor can be installed as the driving source inside the blood vessel, removing the need to transmit rotational motion through a long tortuous blood vessel. This would improve the rotational stability and prevent the shaft of the rotating device from breaking.

Various types of ultrasound motors, including ring motors, linear motors, levitated-rotor motors, and coiled-stator motors have been actively investigated [4] [5] [6] [7]. We have been developing a CS-USM to construct a micromotor [8] [9] [10]. Since the CS-USM has a simple structure compared to other types of ultrasound motors, it is suitable for miniaturization. Ultrasound micromotors with outer circumferences of less than 1 mm have been fabricated using the coiled-stator structure by some groups [8] [11]. The main problem in terms of practical use is its low efficiency. A quadratic driving method using a closed-loop waveguide has been proposed for improving the efficiency [12]. However, the piezoelectric transducers need to be attached to the waveguide, and the acoustic impedances of a closed-loop waveguide are non-uniform at the attachment points. We thus think that these attachment points may cause the low efficiency. Further improvement may therefore be required. We previously proposed a new CS-USM structure that had an ultrasound power circulation-type acoustic waveguide and employed the quadratic excitation method [10]. Furthermore, a connection method between the piezoelectric transducer and acoustic waveguide was proposed to minimize the effect of acoustic propagation characteristics on the acoustic waveguide. in the previous paper [10]. Also, we previously reported a method for measuring the torque of the micromotor and the torque-revolution speed characteristics of the CS-USM [9]. These papers did not deal with the relationship between torque and revolution speed

 ISBN: 978-1-61208-375-9

characteristics and the relationships among torque, output power, and efficiency of a Π-shaped CS-USM. These relationships are described in the present paper.

The remainder of this paper is organized into the following five sections. Section II presents the concept of the CS-USM for IVUS. Section III describes the driving principle of our CS-USM. Section IV shows the fabrication of the Π-shaped CS-USM. Section V describes the measurements of the characteristics of the Π-shaped CS-USM. Finally, Section VI gives our conclusions.

II. CONCEPT OF CS-USM FOR IVUS

Recently, intravascular diagnosis by using IVUS has become widely used in medicine [1]. IVUS is minimally invasive and can reduce pain felt by the patient, and is mainly used for examination of coronary artery disease. Since the size of the drive source for rotating the ultrasound sensor is large in the IVUS systems currently in practical use, it is installed outside the body, and the rotational power for the ultrasound sensor is transmitted through the long tortuous blood vessel. Such systems suffer from the problem that the rotation becomes non-uniform due to overloading of the wire transmitting the rotational power, and the problem that the available time is limited in order to prevent the wire from being damaged due to overload. We thus developed the CS-USM as a miniature ultrasound motor that can be used inside the blood vessels in order to solve these problems. Figure 1 shows a conceptual diagram of the structure of an IVUS system using a small CS-USM for rotating the ultrasound sensor.

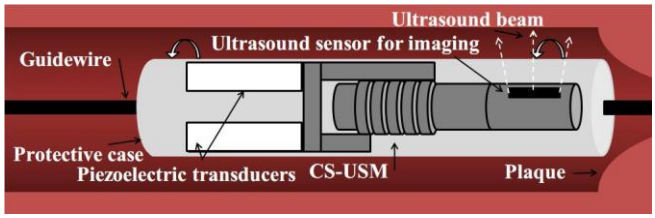

Figure 1. Conceptual diagram showing the structure of an IVUS system using a CS-USM small motor for rotating the ultrasound sensor.

If an ultra-miniature CS-USM can be developed for use inside blood vessels, it is expected that the CS-USM will be able to rotate stably in the blood vessel since there is no need to transfer the rotational power though the long tortuous blood vessel. Furthermore, damage to the wire due to overloading is expected to be prevented.

III. DRIVING PRINCIPLE

In this section, we describe the driving principle of the CS-USM and Π-shaped CS-USM. The driving principle of the CS-USM is described in Subsection A. The driving principle of the Π-shaped CS-USM is detailed in Subsection B.

A. Driving Principle of CS-USM

The CS-USM is a traveling-wave ultrasound motor that uses a coiled stator. When a flexural wave propagates along the coiled stator, particles on the surface of the coiled stator are displaced along an elliptical locus due to the coupling of longitudinal and transverse waves. A rotor arranged inside of the coiled stator is driven in the opposite direction to the particle movement by the frictional force as shown in Figure 2.

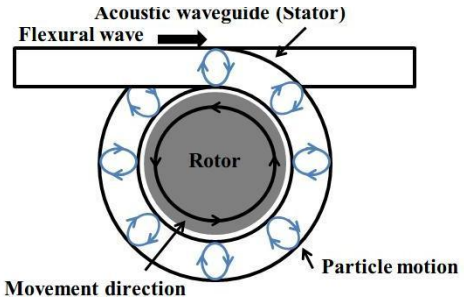

Figure 2. Rotor rotating in the opposite direction to the propagation of the flexural wave in the coiled stator [10].

The CS-USM consists of piezoelectric transducers, an acoustic waveguide, and a rotor. Since it has such a simple structure, it is expected to be able to be miniaturized as an ultrasound motor. Since a coiled acoustic waveguide is used as the stator, driving force is imparted to the rotor along a large part of the interface between the rotor and the stator. That is, even if the stator has a small driving force per unit length, a large drive force can be imparted to the rotor by using a coiled stator [13].

B. Driving Principle of Π-shaped CS-USM

Figure 3 shows the structure of the Π-shaped CS-USM. The motor consists of a rotor, a coiled stator, and two lead zirconate titanate ceramic (PZT)-based piezoelectric transducers. The stator forms a closed acoustic waveguide loop with the coiled waveguide and straight waveguide connected at connection points A and B. The length of the closed-loop waveguide is an integer multiple of the wavelength of the ultrasound wave.

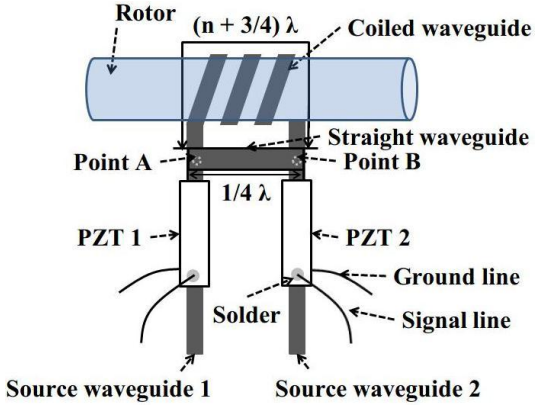

Figure 3. Configuration of our Π-shaped CS-USM [10].

The traveling wave for rotating the rotor can be generated by superposing two standing waves of phases that differ by 90 degrees with respect to both position and time [14]. In the following equations, standing wave (1) is induced at point A by PZT 1, standing wave (2) is induced at point A by PZT 2, and traveling wave (3) is then generated from the two standing waves.

$$u_1(x, t) = A \sin kx \sin \omega t, \quad (1)$$

$$u_2(x, t) = A \cos kx \cos \omega t, \quad (2)$$

$$\begin{aligned} u_t(x, t) &= u_1(x, t) + u_2(x, t) \\ &= A \sin kx \sin \omega t + A \cos kx \cos \omega t \\ &= A \cos(kx - \omega t), \end{aligned} \quad (3)$$

where, A, k, x, ω, and t are the flexural wave amplitude, wavenumber, position, angular frequency, and time, respectively. It is easy to change the rotation direction by switching the phase difference from 90° to -90°.

IV. Fabrication of Π-shaped CS-USM

The fabrication of the CS-USM is described in this section. The structure and design of the Π-shaped CS-USM are described in Subsections A and B, respectively.

A. Structure of Π-shaped CS-USM

As shown in Figure 3, the length of the straight section from point A to point B is λ/4. The length of the closed-loop waveguide including coiled stator from point B to point A in a counterclockwise direction is $(n + 3/4)\lambda$, where n is an arbitrary integer. Source waveguides 1 and 2 are connected to the closed-loop waveguide at connecting points A and B by electric spot welds. The two PZT transducers are attached by soldering to source waveguides 1 and 2, respectively.

B. Design of Π-shaped CS-USM

Figure 4 shows a photograph of the fabricated Π-shaped CS-USM.

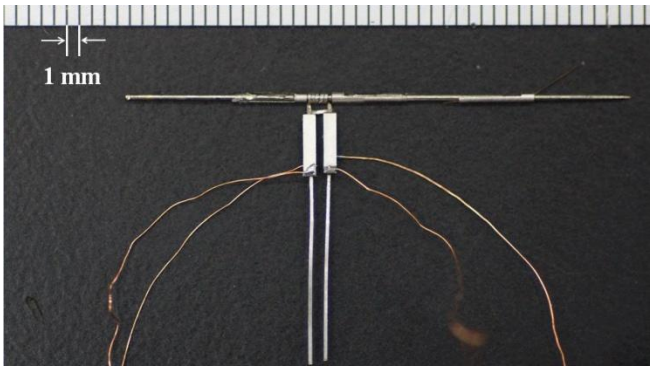

Figure 4. Fabricated Π-shaped CS-USM [9].

The thickness and width of the acoustic waveguides are 0.1 and 0.3 mm, respectively. The material of the acoustic waveguide is SUS 304. The coiled stator is wound 5 turns around the rotor. The thickness, width, and length of the PZT transducer (C-213, Fuji Ceramics) are 0.25, 1.0, and 5 mm, respectively. The rotor is a steel wire with a diameter of 0.56 mm. The inner diameter of the coiled stator is 0.6 mm. The length of the straight waveguide from point A to point B is 1.5 mm. The length of the closed waveguide from point B to point A in a counterclockwise direction is 10.5 mm.

V. Measurement of Characteristics of Π-shaped CS-USM

We measured the characteristics of the Π-shaped CS-USM. Subsections A, B, and C, respectively, describe the following relationships for the Π-shaped CS-USM: the relationship between applied voltage and revolution speed; the relationship between torque and revolution speed; and the relationships among torque, output power, and efficiency.

A. Measurement of Revolution Speed

We measured the revolution speed of the Π-shaped CS-USM by using a laser Doppler velocimeter. The laser beam is reflected by reflective tape attached to the rotor, and the revolution speed is determined from the reflected beam. The Π-shaped CS-USM is held in a CS-USM holder for characteristics measurement as shown in Figure 5. The CS-USM holder is able to hold the rotor, keeping constant contact between the rotor and the coiled stator.

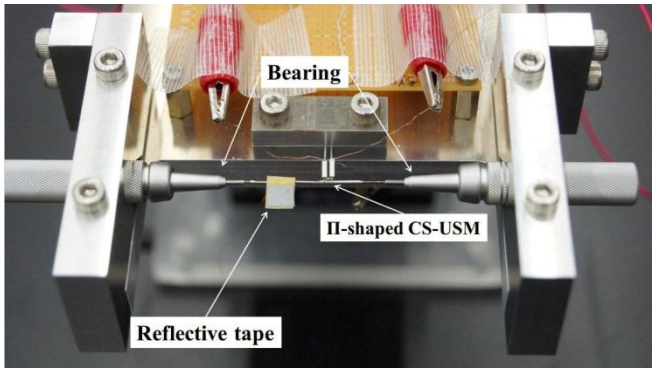

Figure 5. CS-USM holder for measuring characteristics [9].

First, the resonance frequency of the piezoelectric transducers was measured with a fixed voltage applied to the piezoelectric transducers. The resonance frequency of the Π-shaped CS-USM was estimated to be 311 kHz from the results. Next, the revolution speed was measured by sweeping the applied voltage from 2 to 32 V_{pp} at the resonance frequency. Furthermore, the revolution speed and direction of revolution were measured at the resonance frequency after switching the phase difference of the driving signal from 90° to -90°. A continuous sinusoidal wave was used for the driving signal in this experiment.

Figure 6 shows revolution speed as a function of applied voltage. We repeated the measurement of rotational speed 10 times. Mean values with error bars indicating the standard deviation are plotted in Fig. 6.

 ISBN: 978-1-61208-375-9

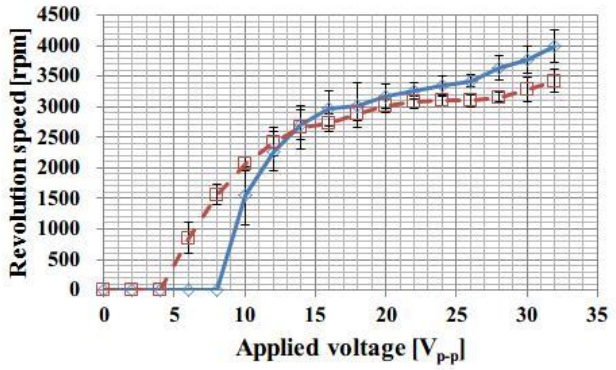

Figure 6. Revolution speed as a function of applied voltage.

It was found that the revolution speed was about 3500 rpm, but it differed between the forward and reverse directions. The forward direction is defined as the direction in which the traveling wave propagates along the coiled stator.

B. Measurement of Torque-Revolution Speed

We next measured the relationship between torque and revolution speed. Figure 7 shows a schematic diagram of the measurement of the torque-revolution speed characteristics, where R, T, W_{tr}, W_{ap}, M_{tr}, M_{ap}, and g are the radius of the rotor, tensile force, true weight, apparent weight, true mass, apparent mass, and gravitational acceleration, respectively. A weight was suspended from the Z stage using a string, and was wound once around the rotor.

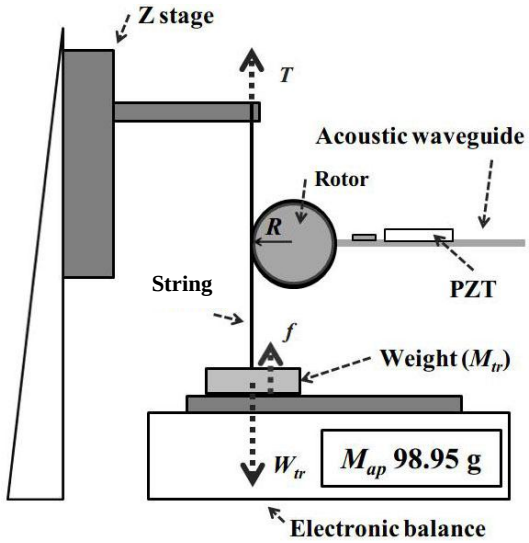

Figure 7. Schematic diagram of measuring torque-revolution speed characteristics [9].

This structure provides a load on the rotor by the movement of the Z stage. At the same time, the revolution speed of the motor was measured using a laser Doppler velocimeter. As in the measurement of the revolution speed, the Π-shaped CS-USM was held by the CS-USM holder while measuring the characteristics as shown in Figure 5. Torque τ is given by (4) as follows:

$$\tau = R \times T. \quad (4)$$

In addition, A and B can be obtained by (5) and (6) as follows:

$$T = W_{tr} - W_{ap}, \quad (5)$$

$$W_{ap} = M_{ap} \times g. \quad (6)$$

The drive conditions were the same as those in the revolution speed measurement. Drive frequency, applied voltage, and drive signal were 311 kHz, 30 V, and continuous wave, respectively. We measured the torque while changing the load on the rotor by moving the Z stage. Figure 8 shows the system for measuring the torque-revolution speed characteristics. Figure 9 shows the revolution speed as a function of torque.

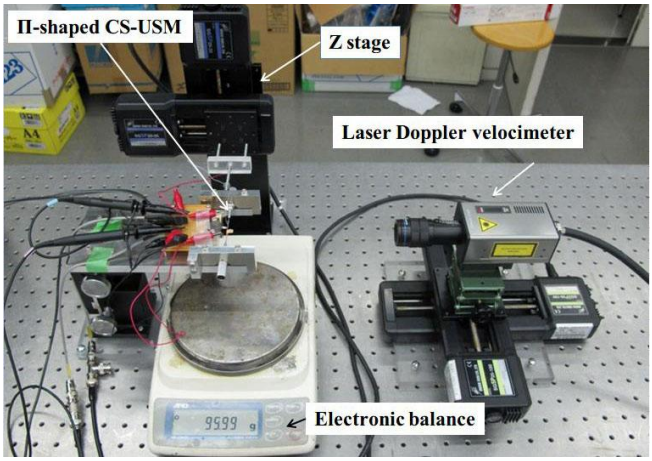

Figure 8. System for measuring torque-revolution speed characteristics [9].

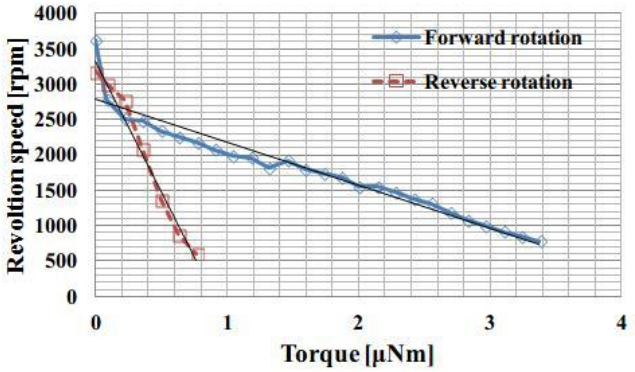

Figure 9. Torque-revolution speed characteristics [9].

It was confirmed that the torque of the Π-shaped CS-USM was about 3.4 μNm and 0.9 μNm in the forward and reverse rotation directions, respectively. The revolution speed decreased with increasing torque. The torque in the forward direction was different from that in the reverse direction.

 ISBN: 978-1-61208-375-9

C. Estimation of Output Power and Efficiency of Π-shaped CS-USM

We calculated the output power of the Π-shaped CS-USM from the torque and rotational speed. We also calculated the efficiency from the torque and rotational speed. In addition, we calculated the efficiency from the output power of the Π-shaped CS-USM and the input power of the PZT transducers. The input power to the PZT transducers taking into account the power factor was 21.6 mW at 30 V_{pp}. The input power required to drive the motor was 43.2 mW. Figure 10 shows the output power and efficiency as a function of torque for forward rotation. Figure 11 shows the output power and efficiency as a function of torque for reverse rotation.

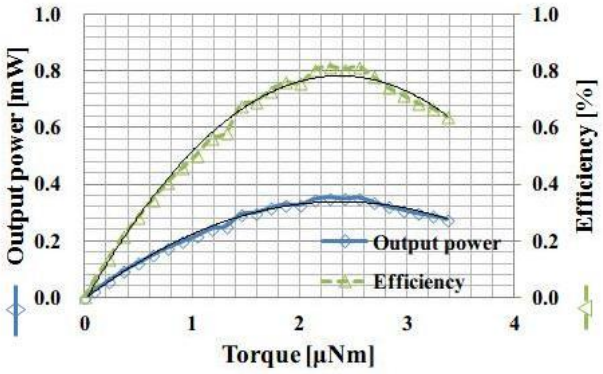

Figure 10. Output power and efficiency as a function of torque for forward rotation

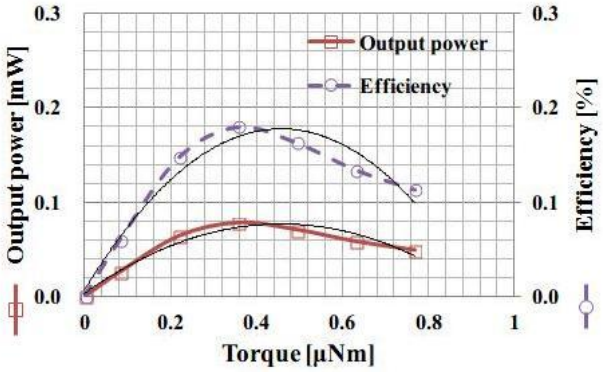

Figure 11. Output power and efficiency as a function of torque for reverse rotation.

The maximum efficiency was thus found to be about 0.8% and 0.2% in the forward and reverse rotation directions, respectively.

VI. Conclusions and Future Work

We fabricated a Π-shaped CS-USM to improve the driving efficiency of CS-USMs for driving IVUS ultrasound sensors. The relationship between the revolution speed and torque of the fabricated Π-shaped CS-USM was measured. The driving efficiencies were calculated from the measurement data. The maximum driving efficiency was confirmed to be about 0.8%. In previous research, the maximum driving efficiency of a large single-transducer CS-USM was found to be about 0.1%. The observed improvement in driving efficiency shows the superiority of the closed-loop acoustic waveguide for Π-shaped CS-USM. However, the fabricated CS-USMs exhibited individual differences in driving frequency, revolution speed, and torque performance. These individual differences may be caused by poor fabrication accuracy and experimental conditions. Therefore, improvement in the manufacturing accuracy of the CS-USM is desired. To use the CS-USM in medicine, miniaturization and biocompatibility are required. Therefore, it is necessary to give sufficient consideration to the components and structure of the CS-USM. Optimization of the thickness and width of the closed acoustic waveguide is a problem for the future.

References

[1] W. B. Keeling, et al, “Plaque excision with the Silverhawk catheter: Early results in patients with claudication or critical limb ischemia,” J. Vasc. Surg., Vol. 45, Jan. 2007, pp. 25-31.

[2] Y. Saijo, A. Tanaka, N. Owada, and S. Nitta, “Tissue velocity imaging of coronary artery by rotating-type intravascular ultrasound,” Ultrasonics, Vol. 42, Apr. 2004, pp. 753-757.

[3] Y. Saijo and A. F. W. van der Steen Eds., “Vascular Ultrasound,” Tokyo: Springer-Verlag, Jul. 2003, p. 57.

[4] T. Maeno, T. Tsukimoto, and A. Miyake, “Finite-element analysis of the rotor/stator contact in a ring-type ultrasonic motor." IEEE Trans. Ultrason. Ferroelectr. Freq. Control., Vol. 39, Nov. 1992. pp. 668-674.

[5] C. H. Yun, T. Ishii, K. Nakamura, S. Ueha, and K. Akashi, “A high power ultrasonic linear motor using a longitudinal and bending hybrid bolt-clamped Langevin type transducer,” Jpn. J. Appl. Phys., Vol. 40, May 2001, pp. 3773-3776.

[6] T. Yamazaki, J. Hu, K. Nakamura, and S. Ueha, “Trial construction of a noncontact ultrasonic motor with an ultrasonically levitated rotor.” Jpn. J. Appl. Phys., Vol. 35, May 1996, pp. 3286-3288.

[7] T. Moriya and Y. Furukawa “Ultrasonic motor.” U.S. Patent No. 7,602,103., Oct. 2009.

[8] T. Abe, T. Moriya, T. Irie, and S. Takeuchi, “Development of Hydrothermally Synthesized PZT Polycrystalline Film Transducers for CS-USM (Coiled Stator Ultrasound Motor),” Res. Bull. TOIN Univ. Yokohama, Dec. 2013, pp. 13-17. (In Japanese)

[9] T. Abe, T. Moriya, T. Irie, and S. Takeuchi, “Characteristic of Π-Shaped Coiled Stator Ultrasound Motor (CS-USM),” ICICE tech. rep, Vol. 114, May 2014, pp. 13-17. (In Japanese)

[10] T. Abe, T. Moriya, T. Irie, M. Sato, and S. Takeuchi, “Experimental study of the Π-shaped coiled stator ultrasound motor,” Jpn. J. Appl. Phys., Vol. 53, Jun. 2014, pp. 07KE15-1-07KE15-5.

[11] A. Nakajima, Y. Furukawa, and T. Moriya, “Development of a New Traveling Wave Ultrasonic Micro Motor : Application to Catheter in Micro Blood Vessels(Nano/micro measurement and intelligent instrument),” Proc. Int. Conf. LEM21, Oct. 2005, pp. 371-374.

[12] K. Youhei, M. Yoshizawa, N. Tagawa, T. Irie, and T. Moriya, “Ultrasonic Power Circulation-type Quadratic Excitation Method for improvement in torque of Coiled Stator Ultrasonic Motor,” Proc. Symp. Ultrason. Electron., Nov. 2012, pp. 475-476.

 ISBN: 978-1-61208-375-9

[13] M. Tanabe, S Xie, N. Tagawa, T. Moriya, and Y. Furukawa, "Development of a Mechanical Scanning-type Intravascular Ultrasound System Using a Miniature Ultrasound Motor," Jpn. J. Appl. Phys., Vol. 46, Jul. 2007, pp. 4805-4808.

[14] K. Uchino and J. R. Giniewicz, "Micromectronics" New York: Marcel Dekker, Apr. 2003, p. 423.